AMER. ZOOL., 38:771–792 (1998)

Muscles, Elastic Energy, and the Dynamics of Body Stiffness in Swimming Eels[1]

JOHN H. LONG, JR.[2]

Department of Biology, Vassar College, Poughkeepsie, New York 12604

SYNOPSIS. **To investigate the capacity of the myomeric muscles to actively change the stiffness of the body during bending, mid-caudal sections (spanning two to three intervertebral joints) of intact, freshly-killed American eels, *Anguilla rostrata,* were dynamically bent (3 Hz, ±4% maximal muscle strain) using the whole-body work-loop technique. Following unstimulated cycles, the left- and right-sides of the musculature were alternately stimulated at supra-maximal voltages and at eight different phases relative to the strain cycle of the muscle. The body's flexural stiffness (Nm^2) increased maximally by a factor of three relative to that when the muscles were unstimulated. The net external work ($J\ kg^{-1}$) needed to bend the body decreased maximally by a factor of seven relative to that when the muscles were unstimulated. Both of these mechanical features varied sinusoidally with changes in the phase of the stimulus. Stimulus phase of caudal muscle in live swimming eels, taken from other studies, leads to the prediction that the caudal muscles increase body stiffness and produce net positive mechanical work simultaneously during steady forward swimming. The association of increased body stiffness and net positive muscle work, and the occurrence of maximal net muscle power output at a stimulus phase of 325° (as the muscle segment lengthens), suggests that net positive power is produced, in part, using an elastic strain energy mechanism.**

INTRODUCTION

In vertebrates, studies of locomotor dynamics have broadened our view of muscle function beyond the classical model of forceful shortening. For example, measurements of muscle activity patterns (electromyography, "EMG") in flying doves suggest that several flight muscles, each formerly classified as either a wing elevator or depressor, operate instead as wing decelerators and accelerators (Dial, 1992). Likewise, EMG studies of swimming fish show that their axial muscle fibers, under some conditions, may be neurally activated as the fiber is lengthened (Altringham *et al.,* 1993; Johnson *et al.,* 1994; Johnston *et al.,* 1995). By forcefully resisting lengthening caused by either adjacent muscles or hydrodynamic loads, active muscle fibers are said to "generate," from their frame of reference, negative work, meaning that they produce a force oriented in the direction opposite to that of their lengthening. Strictly speaking, from the frame of reference external to the fibers, more positive work is required externally to lengthen an activated fiber compared to that needed to lengthen an inactive one. Whichever convention one chooses, muscles that forcefully resist lengthening should, in order to vary undulatory swimming motions, dynamically alter body stiffness (Long *et al.,* 1996; McHenry *et al.,* 1995). This paper examines the extent to which the muscles of fish alter body stiffness, how they do so, and if they do so during swimming.

Using the whole-body work-loop technique, in which a freshly dead and intact fish is bent while its muscles are electrically stimulated *in situ,* active muscle increased the body stiffness of a largemouth bass, *Micropterus salmoides,* by 6%, a value that likely underestimates the capacity for change since only parts of several myomeres were being stimulated (Long and Nipper, 1996). Greater change is expected on the basis of mechanical theory: fish should use their muscles to increase body stiffness

[1] From the symposium *Muscle Properties and Organismal Function: Shifting Paradigms* presented at the Annual Meeting of the Society for Integrative and Comparative Biology, 26–30 December 1996, at Albuquerque, New Mexico.

[2] E-mail: jolong@vassar.edu

several-fold with increasing swimming speeds in order to match their body's natural frequency to the higher tail-beat frequency needed to increase the hydrodynamic rate of working (Long and Nipper, 1996). Because matching the body's natural and driving frequencies reduces the force required to cause a given motion independent of the hydrodynamic load, dynamic tuning of the body's stiffness would substantially reduce the internal resistance to bending. Evidence that the mechanics of swimming work in this manner comes from experimental changes in the body stiffness of swimming sunfish models (McHenry *et al.*, 1995), swimming sunfish bodies driven by electrically-stimulated muscles (Long *et al.*, 1994), and live gar swimming with and without surgically-altered skin (Long *et al.*, 1996).

In order to accurately model undulatory swimming, we must understand the mechanical functions of muscle within the intact body. As demonstrated by single-fiber *in vitro* work loop experiments (Josephson, 1985), the mechanical performance of muscle fibers isolated from fish varies with changes in strain, strain rate, stimulus pattern, fiber type, acclimation temperature, and body position (Altringham and Johnston, 1990; Altringham *et al.*, 1993; Coughlin and Rome, 1996; Coughlin *et al.*, 1996; Curtin and Woledge, 1993*a, b*; Johnson and Johnston, 1991; Johnson *et al.*, 1994; Johnson *et al.*, 1993; 1995; Rome and Swank, 1992; Rome *et al.*, 1993). Missing is how the performance of these fibers changes when they operate as part of the whole body, with its complex muscle architecture (Spierts *et al.*, 1996; Westneat *et al.*, 1993), intra-muscular pressure (Wainwright *et al.*, 1978), variable neural activation (Jayne and Lauder, 1993, 1994, 1995*a, b* 1996), and serial and parallel elastic structures such as backbone (Long, 1992, 1995), skin (Hebrank, 1980; Long *et al.*, 1996), and myotomes (Westneat *et al.*, 1993). In theory, the stiffness, arrangement, and hydrodynamic loading of elastic elements should determine the function of muscle (see Alexander, 1988; Ettema, 1996; Jordan, 1996; Pabst, 1996; compare Bennett *et al.*, 1987 and Blickhan and Cheng, 1994).

In this study I show that the intact mid-caudal myotomal muscle of the American eel, *Anguilla rostrata,* can, when stimulated, triple the body's stiffness compared to the unstimulated body. Furthermore, changes in stiffness are associated sinusoidally with changes in the muscles' net mechanical work, the muscles probably increase body stiffness during steady swimming, and the caudal myomeric muscles may use elastic energy storage to produce positive power.

METHODS

I used American eels for these experiments because they, their European congeners, *Anguilla anguilla,* or other eel-like swimmers have been the focus of studies on undulatory kinematics (Gillis, 1996; Gray, 1933; Williams *et al.*, 1989), neural control of muscle activity (Gray 1936*a, b,* Grillner and Kashin, 1976), hydrodynamics (for review see Lighthill, 1975), and swimming mechanics (Bowtell and Williams, 1991; Hebrank, 1980). Furthermore, during steady swimming it appears that both red and white muscle are simultaneously active on alternating sides of the body (Grillner and Kashin, 1976), a pattern easily mimicked in our whole-body work loop experiments. Female eels were captured in traps in the freshwater region of the Hudson River at the Norrie Point Environmental Site in October and November, 1995. They were held indoors in aquaria for one year with a 12:12 hour light : dark cycle and water temperatures fluctuating from 18 to 22°C. Eels were fed live fish, a diet which required active foraging, thus ensuring daily exercise. Individuals were tested once grown to a size amenable for these experiments (Table 1). Experiments were conducted at 20°C. All procedures in this study were approved by the Institution Animal Care and Use Committee of Vassar College.

I conducted whole-body work loop experiments (Long and Nipper, 1996), which combines techniques from the half-myotome stimulation (Johnsrude and Webb, 1985) and *in vitro* work loop (Josephson, 1985) procedures. Each of the eels was anaesthetized with tricaine (1:10,000 dosage; sold as Finquel, Argent Chemical); then its

spinal cord was transected below the medulla in order to eliminate static undulatory curvature (Gray, 1936*a*). The body was mounted so that a small section of the mid-caudal region—midway between the cloaca and the posterior margin of the caudal fin at a relative axial position of 70% (±1.0%, SD) total body length, L_b, from the tip of the rostrum—was left free to bend laterally (Fig. 1). The mid-caudal region was chosen because these muscles have been implicated in the generation of negative work in some species (see Wardle *et al.*, 1995) and because, in eels, it is one position from which muscle activity patterns were measured (at 72.4% L in a 41.1 cm L eel, Grillner and Kashin, 1976; and at 75% L by G. Gillis, personal communication). The mounts were made of aluminum pipe of 1.56 cm inner diameter; the anterior and posterior sections of the eel's body, relative to the targeted mid-caudal section, were placed into each pipe and were held in place by a pin inserted through holes in each pipe and then through the eel. Lateral movement of the eel was restricted by inserting between the eel and the pipe walls air-injected styrene particles (packing material). The styrene, if compressed while inserted, would expand and hold the eel snugly in place with the gripping force evenly distributed circumferentially and axially. The mounted eel was visually inspected for slippage.

The two mounts were clamped to the oscillating and stationary sections of the dynamic bending machine; the anterior margin of the bending section was aligned with the bending axis (Fig. 1B). This configuration approximates that of a cantilevered beam with a bending couple input at one end (Fig. 1A). At static equilibrium, the flexural stiffness, EI (Nm^2), of the beam is given by the following formula (Stevens, 1987):

$$EI = \frac{CL}{\theta_{max}}, \quad (1)$$

where θ is the angular deflection (° or radians), C is the bending couple (Nm), L is the length of the beam (m), E is the Young's modulus (Nm^{-2}), and I is the second moment of area (m^4). The two latter terms represent the contributions of material and shape, respectively, and are therefore often measured and reported as the composite, EI, for anisotropic, heterogeneous structures.

The body section was bent sinusoidally at a frequency of 3 Hz, which corresponded in similarly sized eels to tailbeat frequencies used during steady swimming (W. Shepherd, personal communication). Collinear with the bending axis was an angle sensor (RVDT, rotary variable differential transducer, Shaevitz model R30D); the bending moment, M (Nm) transmitted through the test section was transduced using two foil strain gauges (Omega Engineering, 120 Ω) mounted on the cantilevered steel support of the stationary grip (Fig. 1B). This half-bridge configuration was excited at 5 VDC using a 40 kHz bridge amplifier (Omega Engineering, model DMD-520). The bending moment transducer was calibrated by inputting a series of known static moments. The dynamic measurements (described below) were always greater than 90% accurate, as tested using a homogeneous beam (polyvinyl chloride) of known mechanical properties.

In all experiments, I adjusted the testing conditions to produce a maximal linear strain, ε (ratio of minimum or maximum lateral length of the bent body to length of the straight body), of approximately ±4% for the superficial muscle in the test section (Table 1). A maximal ε of ±4% is within the maximum range estimated for white muscle during unsteady swimming (Franklin and Johnston, 1997; Johnston *et al.*, 1995; Johnson *et al.*, 1994), is within the maximal range used in studies of superficial red muscle (Swank *et al.*, 1997), and is only slightly smaller than the value of ±6% used to model *in vivo* swimming power in posterior white muscles (Rome *et al.*, 1993). To produce an ε of ±4% for eels of different body widths, D_w (m), given a constant angular strain of θ ± 4.25° in the bending machine, I used the following equation, which calculates ε as a function of the ratio of the lateral-to-midline radii of curvature (Johnson *et al.*, 1994):

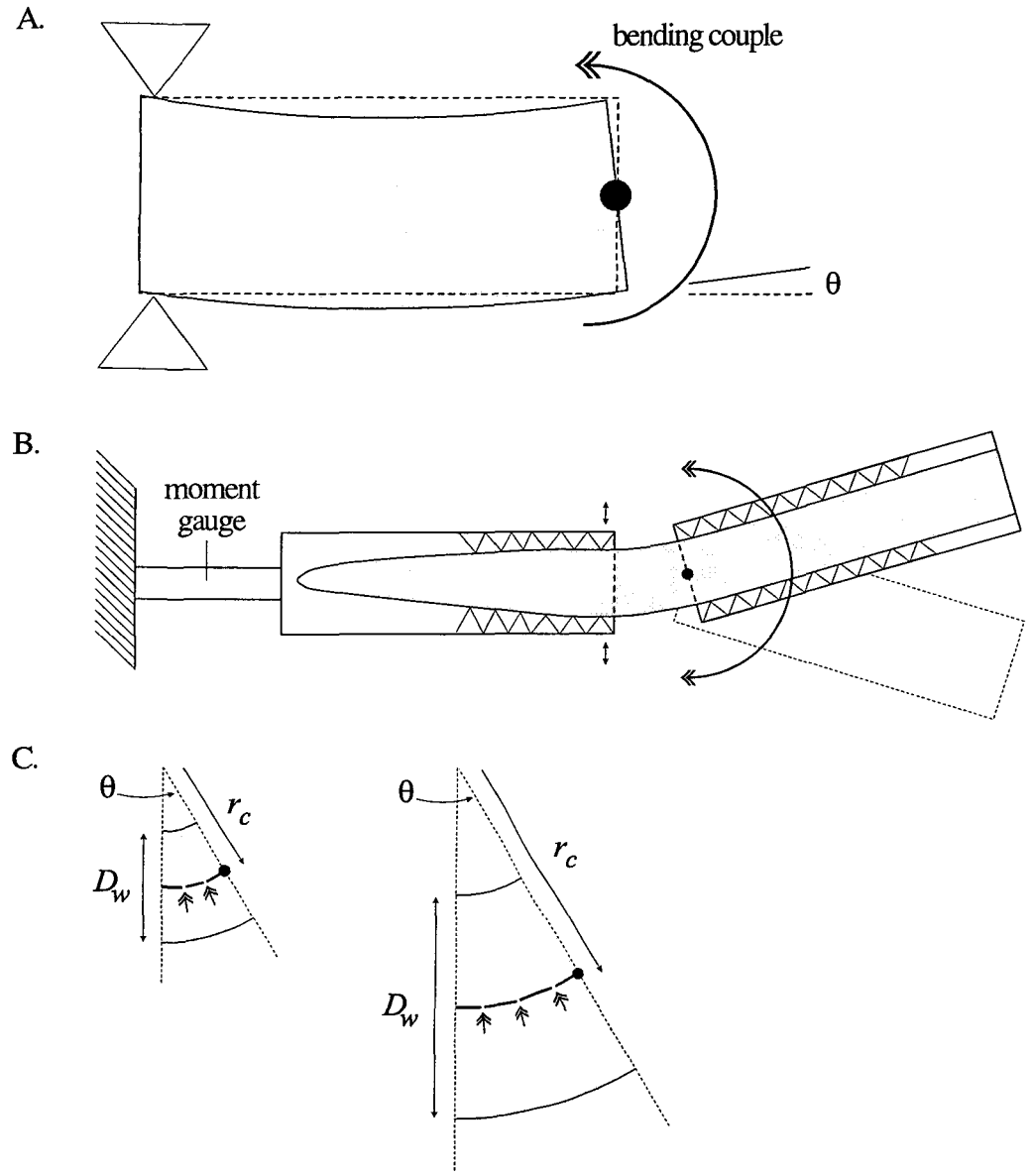

FIG. 1. Whole-body work-loop experiments. A. Mechanical analogue for bending conditions. One end of the beam is held rigidly, while the other rotates when torqued by a bending couple. The resulting angular displacement, θ, is a function of the beam's length and flexural stiffness (see eq. 1). B. Diagrammatic view of the bending machine. A cantilevered moment gauge is attached to a grip that holds the tail of the eel (to the left). The anterior portion of the eel (to the right) is held in a grip that oscillates about the bending axis (black dot). The bending couple (large double-headed arrow) causing the oscillation is transmitted through the bending section resulting in a bending moment measured by the gauge. A small deflection (maximum of ±1 mm) of the stationary grip (small double-headed arrows) results in a negligible acceleration of the tail's grip (see Methods). C. To maintain a constant superficial muscle strain, ε (±4%) and bending angle, θ (±4.25°) in eels of different body widths, D_w, the length of the test section was varied (see eq. 2). The test section of the smallest eel (left figure; #1 in Table 1) thus differed from that of the larger eels (right figure; #2 & #3 in Table 1), containing only two intervertebral joints (double-headed arrows) and experiencing greater curvature, κ (m^{-1}), the inverse of the radius of curvature, r_c figured here.

TABLE 1. *Morphological features of the experimental eels and their bent body sections.*

Feature	Eel 1	Eel 2	Eel 3	Mean (±SD)
L_b, total length (m)	0.21	0.30	0.33	0.28 (0.063)
Total weight (kg)	0.0073	0.0371	0.0573	
Axial position of test section (% L_b)	0.71	0.69	0.70	0.70 (0.010)
Intervertebral joints in test section	2	3	3	
θ_j, maximal flexion of joints (°)	2.125	1.417	1.417	
L_v, length of section vertebrae (m)	0.00185	0.00290	0.00280	
D_w, transverse width of body (m)	0.0038	0.0086	0.0087	
ε, maximal strain of superficial muscle (% resting length)	3.81	3.67	3.84	3.77 (0.093)
L_t, axial length of test section (m)	0.0039	0.0075	0.0081	
Maximal curvature of midline (m^{-1})	38.0	19.8	18.3	
Dorso-ventral height of section (m)	0.0080	0.0129	0.0149	
Transverse area (elliptical) ($m^2 \times 10^{-5}$)	2.39	8.71	10.18	
Volume of test section ($m^3 \times 10^{-7}$)	0.93	6.53	8.25	

* Means (± standard deviation) are given only for those features I attempted to hold relatively constant across individuals.

** Other features are used in calculations or for normalizing experimental response variables.

$$\varepsilon = 100\left[\frac{(L_v/(2 \sin \theta_j)) - (D_w/2)}{(L_v/(2 \sin \theta_j))}\right], \quad (2)$$

where L_v is the average length (m) of the vertebrae in the section and θ_j (°) is the maximal flexion of any single joint (the quotient of θ and the number of intervertebral joints in the section; for values, see Table 1). While this kept ε constant across individuals, the resulting maximal midline curvature, κ (m^{-1}), the inverse of the radius of curvature, r_c (m), ranged from 38, 20, to 18 m^{-1} (Table 1). The number of intervertebral joints and the length and orientation of vertebrae within the bending section were verified by dissection after the experiments. Dissection revealed that individual myomeres spanned at least six intervertebral joints and five complete vertebrae. Thus the test sections did not include any complete muscle segments.

Once mounted, the left and right sides of the eel's body were implanted with a pair of platinum stimulating electrodes possessing tips of 1.1 cm in length (Grass Instruments, model E2). On each side the cathode and anode were separated by the maximal distance allowed by the test section length, L_t (Table 1), were oriented parallel to the vertical septum, and provided a linear electrode exposure to the muscle equal to approximately the dorso-ventral height of that section of the body (Table 1). Preliminary experiments showed that this electrode arrangement produced maximal bending moments. Furthermore, ipsilateral myomeres adjacent to those in the test section were stimulated by current leakage, which was responsible, in part, for the two full cycles of supra-maximal stimulation required to achieve a stable and fully potentiated functional state (Fig. 2). The contralateral electrode pairs were supplied independently by two 300 milliamp stimulators (Grass Instruments, model S48). Each stimulator was externally triggered, alternately, by a two-channel, digital stimulator (Grass Instruments, model S11B) with quartz timing circuits. The digital stimulator was in turn externally triggered by a pulse generator (Data Dynamics, model 5113) triggered by the angle sensor attached to the bending machine.

Contralateral myomeric muscle, including all of the red and white fibers, was alternately stimulated for 50% of the bending cycle with an 80 Hz train of electrical pulses of 2 msec duration. The duty cycle of 50% was the maximum value reported for European eel (Grillner and Kashin, 1976); single-fiber work loop studies have used similar train pulses (Johnson and Johnston, 1991). As the experiments proceeded, voltage of the stimulus was increased from 2 to 40 VDC to maintain supra-maximal contraction. The primary independent variable

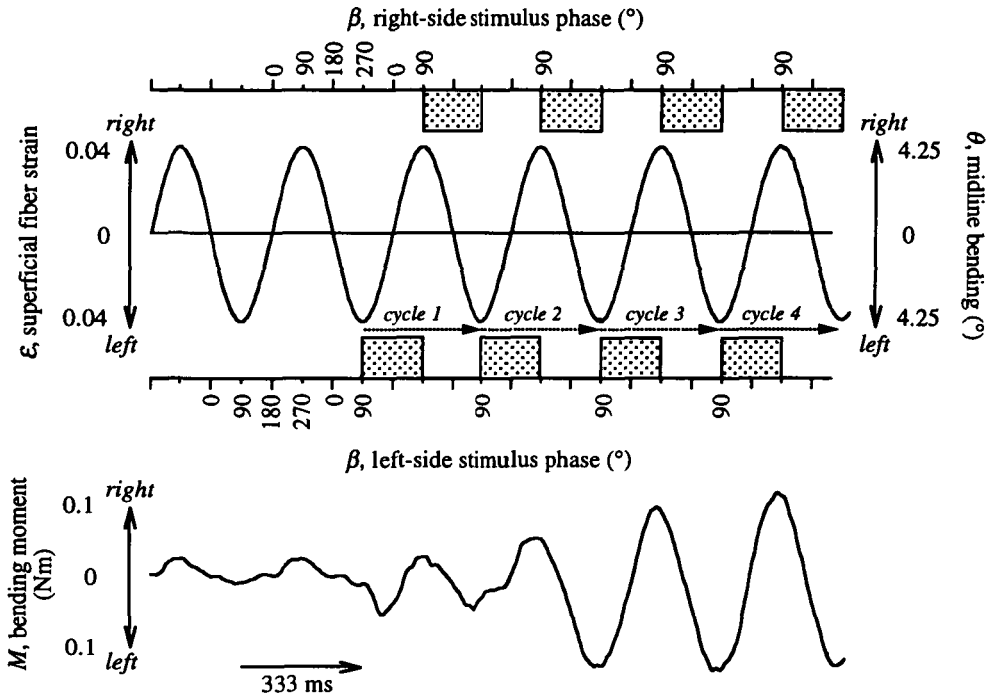

FIG. 2. Typical dynamic signals generated during a whole-body work loop experiment. At a frequency of 3 Hz (333 msec per cycle), a θ of ±4.25° of the body's midline strains superficial fibers ±4%. Electrical stimuli (stippled rectangles) were applied alternately to the left and right sides for 50% of a bending cycle. The stimulus phase, β, was 90°. Stimulation caused the bending moment, *M*, to increase. By the third stimulus cycle, a relatively stable mechanical signal was generated by the fully-potentiated muscle system.

was stimulus phase, β (°), which determines the timing of the onset of the electrical stimulus relative to the axial strain on that side of the body (Fig. 2). Following the convention of single-fiber studies (see Johnson and Johnston, 1991), β = 0° represents the relative time in the bending cycle (a full cycle = 360°) when the onset of electrical stimulation begins as the muscle is at its resting length and is lengthening; β = 90° represents the relative time when the stimulus onset occurs as the muscle is at its maximum length; β = 180° represents the relative time when the stimulus onset occurs when the muscle is at resting length and is shortening; β = 270° represents the relative time when the stimulus onset occurs when the muscle is at its minimum length.

Because the muscle fatigued within one hour, the experiments were performed in two stages, with the most important experiments first. In stage one, I measured the isometric properties of the right and left-side myomeres at supra-maximal voltage with the body held straight. This was immediately followed by sinusoidal bending of the body with electrical stimulation of the muscles at β of 0°, 90°, 180°, and 270°, with the order randomized for each eel to avoid artifacts of test order. In stage two, the new supra-maximal voltage, required because of gradual muscle fatigue, was determined and a second isometric test was performed. This was immediately followed by sinusoidal bending of the body with electrical stimulation of the muscles at β of 45°, 135°, 225°, and 315°, with the order of the phases randomized for each eel to avoid artifacts of test order.

In order to determine the effects of β on the mechanical response variables (see below), two replicates were taken from each experiment (where an experiment is a test at one of eight β values on one of three individuals), yielding a sample size of 48.

Replicates were the third and fourth stimulus cycles; these cycles were chosen because the first two stimulus cycles were required to achieve a stable, fully-potentiated state (Fig. 2). Stimulation was discontinued as soon as possible after the fourth stimulus cycle to prolong the experimental life of the whole-body preparation.

For a dynamically bending beam, whose motion is described by a single degree of freedom, the instantaneous external bending moment, M (Nm), transmitted through the test section is balanced by the sum of the internal moments caused by stiffness, damping, and the change in angular momentum (Den Hartog, 1956; Denny, 1988):

$$M = k\theta_0\sin(\omega t - \delta) + c\omega\theta_0\cos(\omega t - \delta) - N\omega^2\theta_0\sin(\omega t - \delta) \quad (3)$$

where k is the angular stiffness (Nm rad^{-1}), ω is the angular frequency (rad s^{-1}), t is the time (sec), δ is the phase advance of M relative to θ (rad), c is the damping coefficient (kg m^2 rad^{-2} s^{-1}), and N is the moment of inertia (kg m^2 rad^{-3}). Since the moment gauge is mounted on the cantilevered side of the bending machine, the tip of which oscillates at a maximum of ± 1 mm (Fig. 1B), moments due to angular acceleration are negligible, with maximal values of 3.4×10^{-5} Nm (when the effective $N = 1.28 \times 10^{-6}$ kg m^2 for the largest eel, $\omega = 18.85$ rad s^{-1}, and $\theta_0 = 0.074$ rad). Hence eq. 3 simplifies to

$$M = k\theta_0\sin(\omega t - \delta) + c\omega\theta_0\cos(\omega t - \delta). \quad (4)$$

Given the sinusoidal nature of M with respect to t (unstimulated and potentiated cycles in Fig. 2),

$$M = M_0\sin(\omega t) \quad (5),$$

where M_0 is the amplitude (Nm), which was measured from the digitized transducer record (1,000 Hz sample rate) for each experiment (a given β, stimulus state, and individual). In addition, the phase advance, δ (rad), was measured as the relative timing of the peaks of the M and θ signals. To solve for k, a time, t, was found when

$$\cos(\omega t - \delta) = 0 \quad (6)$$

and

$$\sin(\omega t - \delta) = 1 \quad (7),$$

such that the damping term (in eq. 4) was 0; then eq. 4 was combined with eq. 5 to yield

$$k = \frac{M_0\sin(\omega t)}{\theta_0}. \quad (8)$$

To normalize for the different sizes of eels (see Table 1), I substituted eq. 8 into eq. 1, since k is the ratio of M and θ, and replaced the bending couple, C (Nm), with the bending moment, M (Nm). This yielded the flexural stiffness, EI (Nm^2), which takes the subscript "ext" to denote that the bending machine measured the *external* moment working to bend the eel:

$$EI_{ext} = kL_t \quad (9),$$

where L_t is the length of the test section. Likewise, to solve for c, a time, t, was found when

$$\sin(\omega t - \delta) = 0 \quad (10)$$

and

$$\cos(\omega t - \delta) = 1 \quad (11),$$

such that the stiffness term (in eq. 4) was 0; then eq. 4 was combined with eq. 5 to yield

$$c = \frac{M_0\sin(\omega t)}{\omega\theta_0}. \quad (12)$$

To normalize for different sizes, I divided c by L_t, since increases in L_t will increase the lateral velocity of the test section and c is inversely proportional to angular velocity (see eq. 12):

$$c_{ext} = \frac{c}{L_t}. \quad (13)$$

Finally, the external work, W (J), done by the machine on the test section was calculated as a function of the phase advance, δ (in ° or rad) (Den Hartog, 1956):

$$W = \pi M_0\theta_0\sin\delta \quad (14),$$

To normalize for the different muscle masses, m_m (kg), of the various test sections (estimated from test section volume assuming a muscle density of 1,000 kg m^3, Table 1), the following mass-specific work, W_{ext} (J kg^{-1}), was computed:

$$W_{ext} = \frac{W}{m_m}. \quad (15)$$

Two additional indices of each response variable were calculated. To isolate the *absolute* contribution of the stimulated muscle to the fully potentiated state, the difference between the values for the stimulated and unstimulated states was calculated for each β and individual (denoted by EI_{diff}, c_{diff}, and W_{diff}). To determine the *relative* contribution of the stimulated muscle, the ratio of the difference value, EI_{diff} for example, to the unstimulated value, EI_{ext}, was calculated for each β and individual (denoted by EI_{rel}, c_{rel}, and W_{rel}).

During cyclic bending experiments, changes in β were expected to produce sinusoidal changes in net muscle work (Johnson and Johnston, 1991) and hence in all of the dependent variables. Using the mean value of each relative response variable at a given β (n = 8, pooled across individual), a sinusoidal, least-squares regression line was produced which maximized the coefficient of determination (r^2 value), using a nonlinear model of the following form (Systat statistical software, Wilkinson, 1989):

$$y = b + a \sin(\beta + \delta) \quad (16),$$

where y is the response variable, b is the grand mean of the y values (offset of the baseline in units of the response variable), a is the amplitude (units of response variable), β is the stimulus phase (°), and δ is the phase advance (°).

In order to understand the dynamic relationship between the muscularly-generated changes in flexural stiffness, EI_{rel}, and mechanical work, W_{rel}, the sinusoidal functions for the two properties were combined in a parametric plot, with β as the parameterized independent variable. In order to compare the muscular power output of the eel to that of different species and measurement techniques, the externally measured W_{diff} was converted to muscular power output, P_m, (W kg^{-1}) as the product of W_{diff} and the bending frequency (3 Hz). In order to signify that the power was produced by the muscle, and not by the bending machine, the sign of W_{diff} was reversed.

In the isometric tests, the body was held straight and stationary while being stimulated on the right side. The supra-maximal stimulus was identical to that used in the dynamic tests at a bending frequency of 3 Hz. The activation delay (msec), from the onset of the electrical stimulus to the onset of detectable M, was measured, as was the time to the maximal M, M_{max}, and the relaxation time to 50% of M_{max}. The sample size was three, with one trial used from each of the three eels.

RESULTS

When the mid-caudal muscle of eel is maximal stimulated, regardless of the relatively timing of the stimulus, the flexural stiffness, EI_{ext}, of the body increases (Fig. 3A). The difference between the values of EI_{ext} when the muscle is stimulated and unstimulated, EI_{diff}, reveals a pattern of variable changes in body stiffness (Fig. 3B). This pattern is clarified when the changes in EI_{diff} are examined relative to those of the unstimulated body, EI_{ext} (Fig. 3C). The sinusoidal fit of the means of EI_{rel} to β (Fig. 3C), yielded (n = 8, r^2 = 0.716, P = 0.023):

$$EI_{rel} = 1.347 + 1.00 \sin(\beta + 143°) \quad (17).$$

The stimulus phase, β_{max}, that produces the maximal change in EI_{rel}, is 307°; β_{min} occurs at 127°. The maximal EI_{rel} of 2.35 predicted by eq. 17 represents a tripling of the EI of the body caused by muscle stimulation (recall that a relative change of 0 represents no change).

Unlike the flexural stiffness, the damping of the body varies only at some values of β (Fig. 4A). When the muscle is unstimulated, c_{ext} is positive; when the muscle is stimulated c_{ext} either stays approximately the same or decreases, as indicated by the values of c_{diff} (Fig. 4B). The relative changes in damping of the body are indicated by the sinusoidal fit of the means of c_{rel} to β (Fig. 4C), which yielded the following equation (n = 8, r^2 = 0.779, P = 0.008):

$$c_{rel} = -1.33 + 5.13 \sin(\beta + 304°) \quad (18).$$

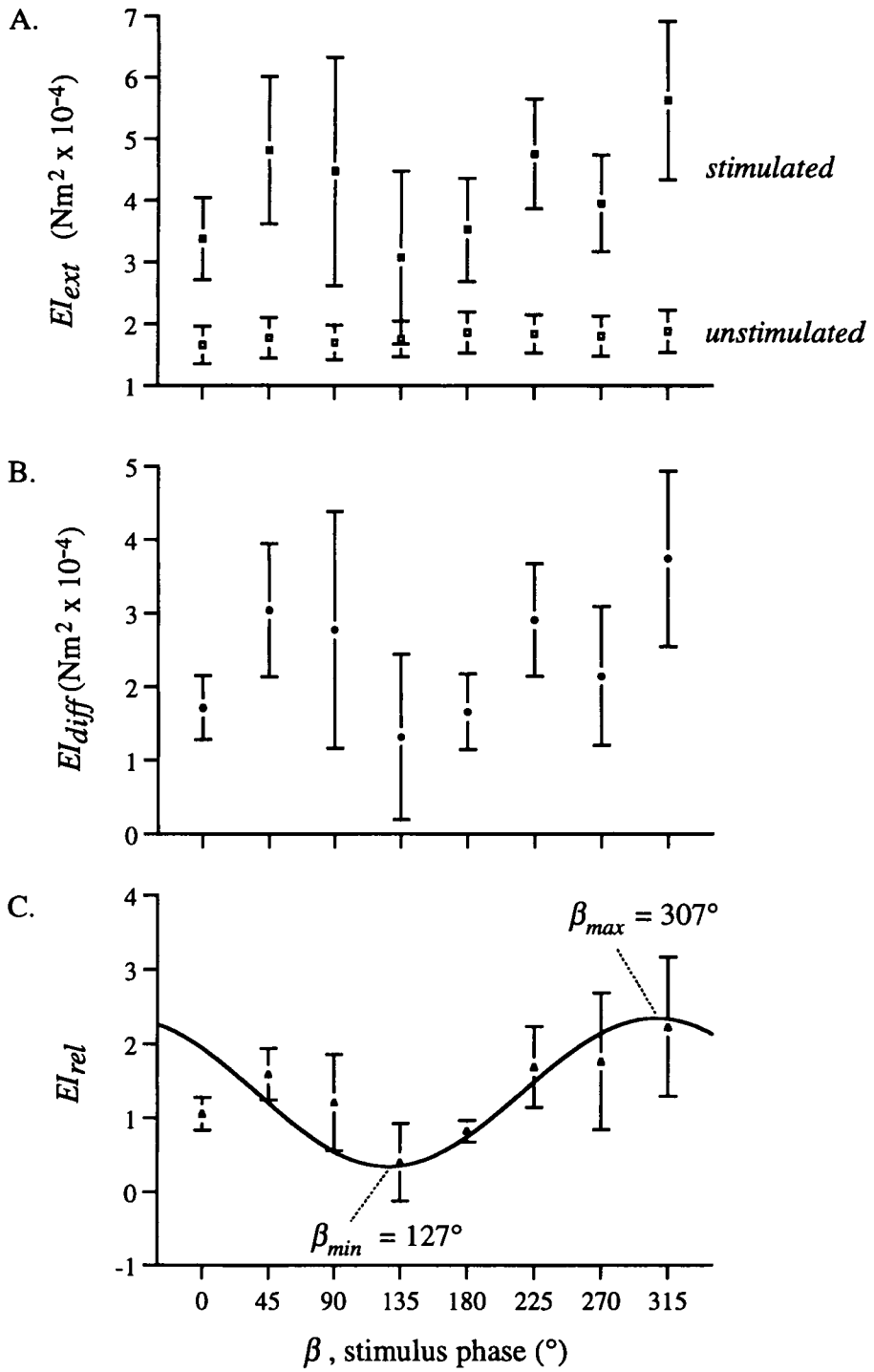

FIG. 3. Flexural stiffness, *EI*, varies with stimulus phase, β. A. When the muscle is stimulated the mean of EI_{ext} increases at each β relative to the unstimulated mean value. B. The contribution of muscle to the stimulated EI_{ext} is indicated by EI_{diff}, the difference of the stimulated and unstimulated values. C. Changes in EI_{diff} relative to the unstimulated EI_{ext} are given as the ratio of the two, EI_{rel}. The line is a least-squares, sine wave regression (see Results for details). Each symbol represents the mean (±SE) of six samples (two replicates for three individuals).

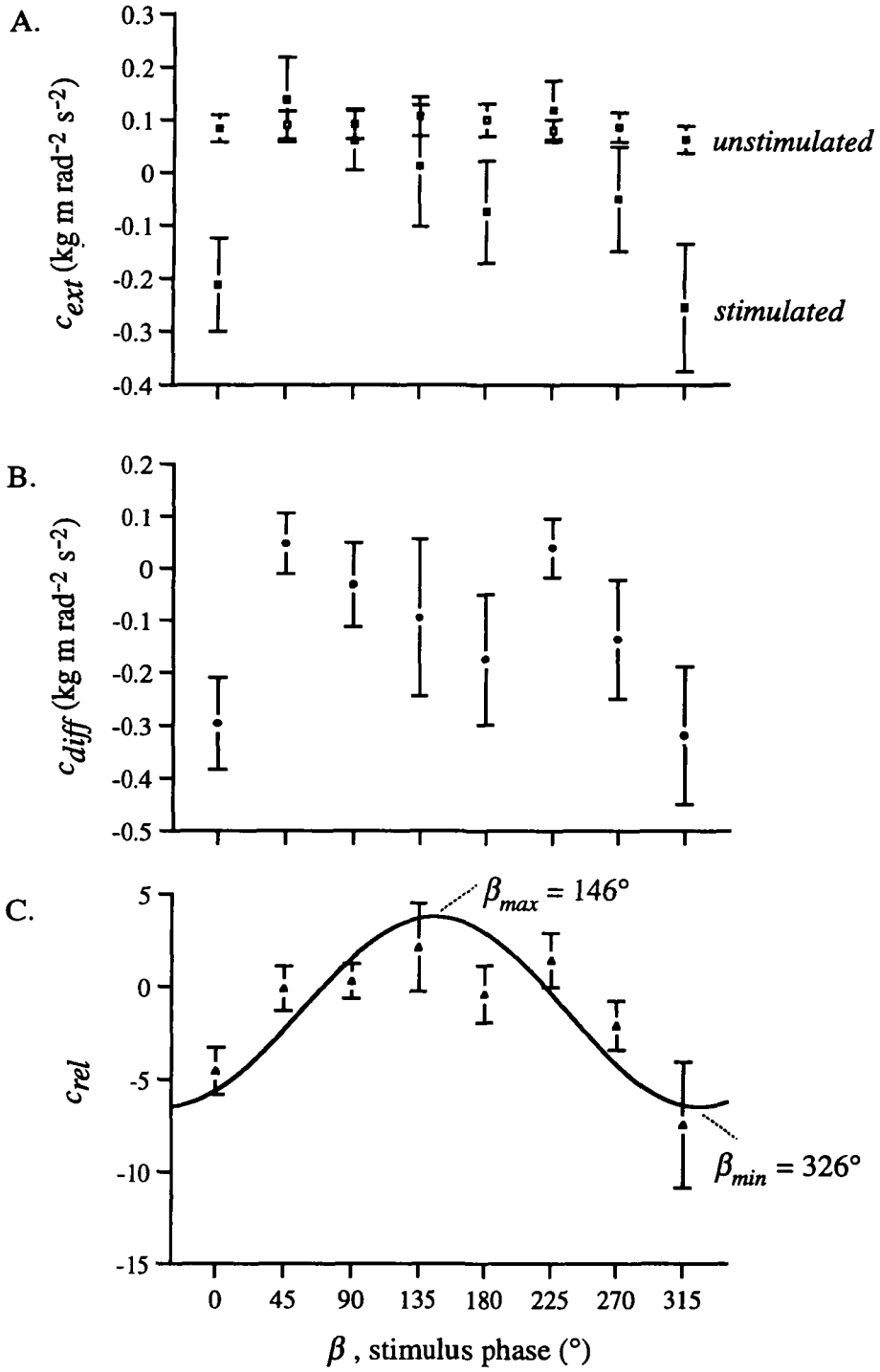

FIG. 4. Damping coefficient, c, varies with stimulus phase, β. A. When the muscle is stimulated the mean of c_{ext} at β of 0° and 315° appears to decrease relative to the unstimulated mean value. B. The contribution of muscle to the stimulated c_{ext} is indicated by c_{diff}, the difference of the stimulated and unstimulated values. C. Changes in c_{diff} relative to the unstimulated c_{ext} are given as the ratio of the two, c_{rel}. The line is a least-squares, sine wave regression (see Results for details). Each symbol represents the mean (±SE) of six samples (two replicates for three individuals).

The stimulus phase, β_{max}, that produces the maximal change in c_{rel}, is 146°; β_{min} occurs at 326°. The minimal and maximal values of c_{rel} of −6.46 and 3.80, respectively, predicted by eq. 18 represent an order of magnitude change in damping caused by the muscles.

The external work, W_{ext}, required to bend the body varies only at some values of β (Fig. 5A). When the muscle is unstimulated, W_{ext} is positive; when the muscle is stimulated W_{ext} either stays approximately the same or decreases, as indicated by the values of W_{diff} (Fig. 5B). The relative changes in the work done to bend the stimulated body are indicated by the sinusoidal fit of the means of W_{rel} to β (Fig. 5C), which yielded the following equation (n = 8, r^2 = 0.779, P = 0.008):

$$W_{rel} = -1.33 + 5.13 \sin(\beta + 304°) \quad (19).$$

Please notice that eqs. 18 and 19 are identical; this is not surprising given that both c_{rel} and W_{rel} are measures of the proportion of M in phase with the angular velocity. The stimulus phase, β_{max}, that produces the maximal change in W_{rel}, is 146°; β_{min} occurs at 326°. The minimal and maximal values of c_{rel} of −6.46 and 3.80, respectively, predicted by eq. 18 represent an order of magnitude change in the work needed to bend the body. Note that a negative value of relative external work indicates that the muscle is performing positive mechanical work. Thus the muscles are capable of generating seven times the work needed to bend the unstimulated body.

To understand the relation between EI_{rel} and W_{rel}, the two functions (eqs. 17 and 19) were combined (Fig. 6). A maximal EI_{rel} of 2.3 occurred at a β of 307°, and a minimal EI_{rel} of 0.3 occurred at a β of 127°. A maximal W_{rel} of 3.8 occurred at a β of 146°, and a minimal W_{rel} of −6.5 occurred at a β of 326°. Thus maximal EI_{rel} is expected when W_{rel} is nearly minimal.

When W_{diff} (Fig. 5B) was converted to muscular power output, P_m (W kg^{-1}), a sinusoidal curve was fit to the mean values at each β (n = 8, r^2 = 0.644, P = 0.070):

$$P_m = 5.64 + 17.50 \sin(\beta + 125°) \quad (20).$$

Even though this regression is only marginally significant (P = 0.07), it yields a phase advance, δ, of 125° (Fig. 7) that is within one degree of the δ, (124°, converted from δ = 304° by subtracting the 180° phase shift caused by changing the sign of the external work) from the highly significant W_{rel} regression (P = 0.008, eq. 19). For comparison with *in vitro,* single-fiber values, I estimated the sinusoidal function of sculpin white muscle from reported values of β at which maximal and minimal P_m occurred (see Fig. 3A of Johnson and Johnston, 1991):

$$P_m = -5 + 25 \sin(\beta + 60°) \quad (21).$$

Both functions were compared to one with an amplitude intermediate to those in eqs. 20 and 21:

$$P_m = 21.25 \sin(\beta) \quad (22).$$

Inspection of these equations (see also Fig. 7) reveal two functionally significant differences: (1) The maximal P_m of eel muscle *in situ* occurs at a δ more than twice that of the maximal P_m of sculpin muscle *in vitro*; (2) in spite of a lower amplitude of the P_m function of eel muscle *in situ* compared to than that of sculpin muscle *in vitro* (17.50 *vs.* 25 W kg^{-1}), the maximal P_m of eel is only slightly greater than that for sculpin (23.14 *vs.* 20 W kg^{-1}).

Results of the isometric tests show that the whole-body preparation delays its onset of contraction from time of stimulation by 17 msec, requires 139 msec to reach maximal bending moment, and relaxes to 50% of the maximal moment in 330 msec, after reaching a maximal bending moment of 0.02 Nm (Table 2).

DISCUSSION

The mid-caudal myomeric muscles of eel, when maximally stimulated during sinusoidal bending, can *triple* the body's flexural stiffness, EI_{rel} (Fig. 3C). These dynamic changes in EI_{rel} are associated with changes in the net work done to bend the body, W_{rel} (Fig. 6). Combined with *in vivo* muscle activity patterns (Gillis, personal communication), whole-body workloops predict that live eels use their caudal locomotor muscle to increase EI_{rel} and

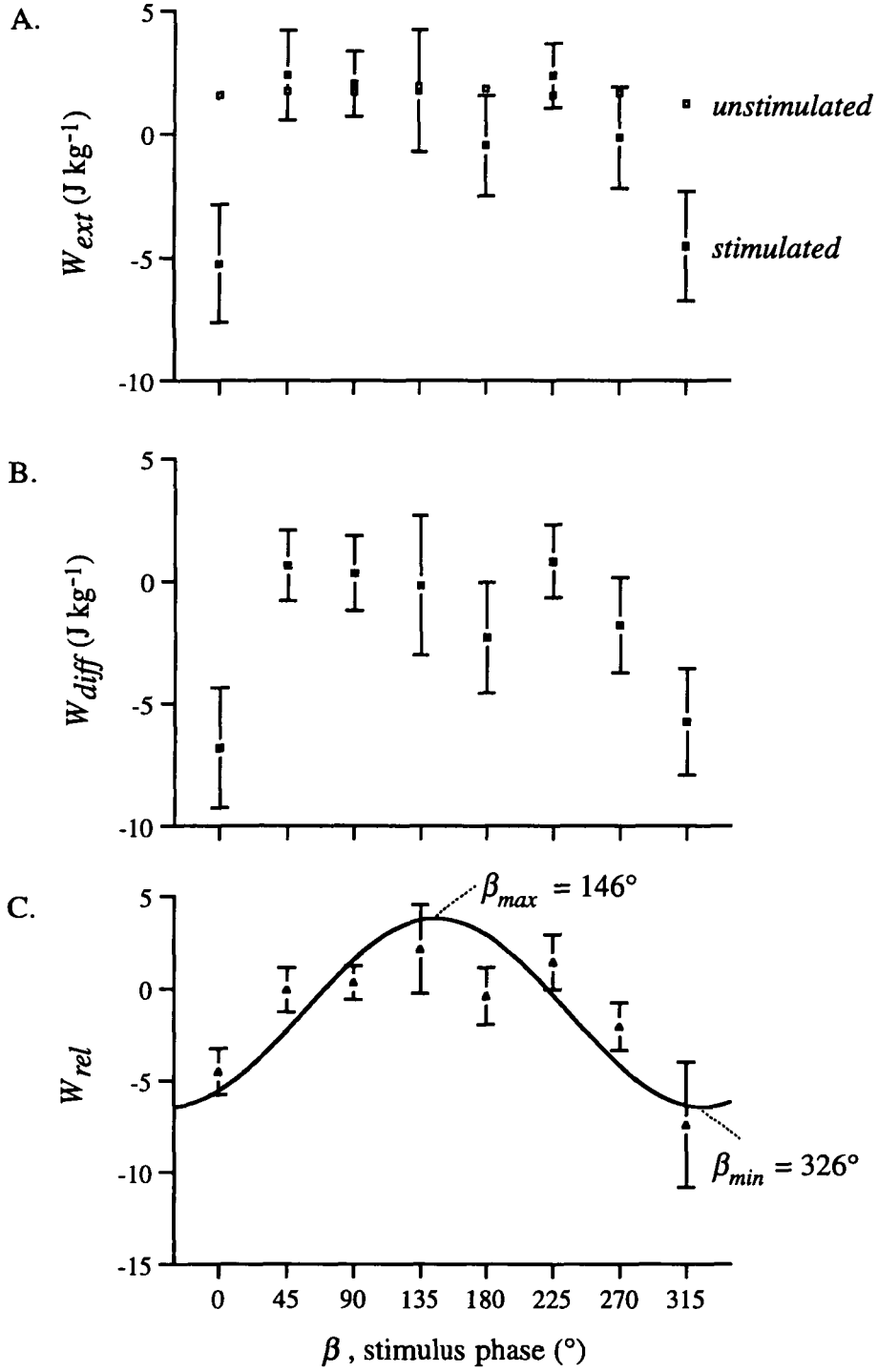

FIG. 5. Mechanical work, W, varies with stimulus phase, β. A. When the muscle is stimulated the mean of W_{ext} at β of 0° and 315° appears to decrease relative to the unstimulated mean value. B. The contribution of muscle to the stimulated W_{ext} is indicated by W_{diff}, the difference of the stimulated and unstimulated values. C. Changes in W_{diff} relative to the unstimulated W_{ext} are given as the ratio of the two, W_{rel}. The line is a least-squares, sine wave regression (see Results for details). Each symbol represents the mean (±SE) of six samples (two replicates for three individuals).

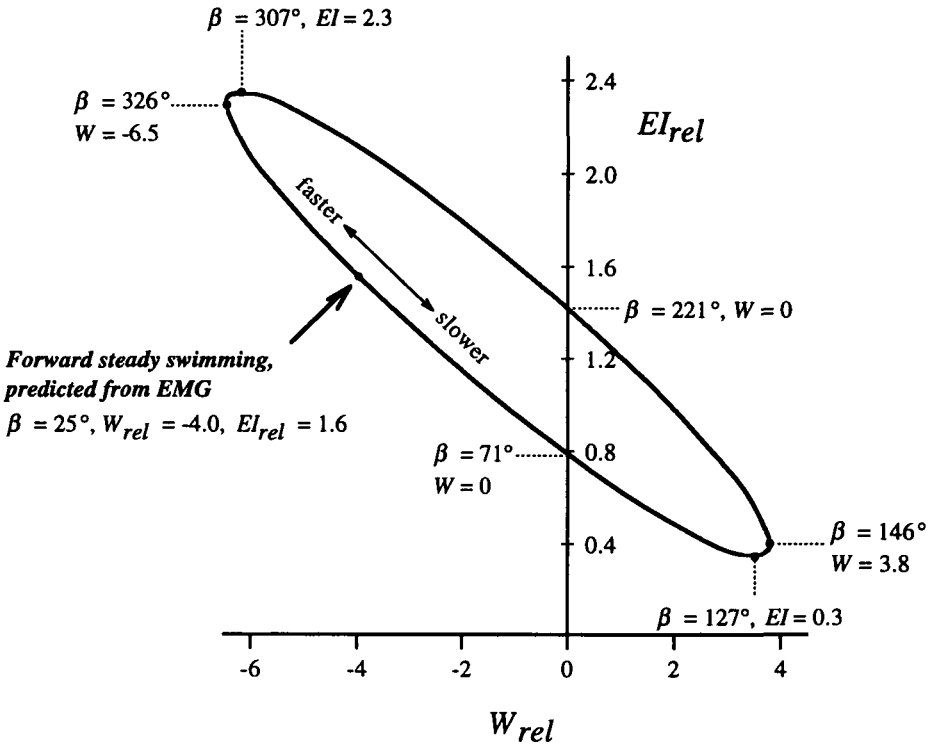

FIG. 6. Dynamics of the whole-body muscle preparation and predicted *in vivo* mechanics. A parametric plot of the sinusoidal function of flexural stiffness, EI_{rel} (see eq. 17) against that of the mechanical work, W_{rel} (see eq. 19), showing how the two are related at any given stimulus phase, β. During steady swimming at 1 L_b sec^{-1} (35–40 cm total length), caudal muscle (at 0.75 L) of eel is activated at a β of 25° (G. Gillis, personal communication). Change in swimming speed may be modulated by increasing (slower swimming) or decreasing (faster swimming) β. Please keep in mind that W_{rel} is measured externally; hence negative values here indicate positive muscle work internally.

to decrease W_{rel} at steady swimming speeds (Fig. 6). In order to produce maximal net positive power (Fig. 7), muscles *in situ* must be stimulated earlier in the lengthening phase (stimulus phases, β, of 325° *vs.* 30°) than those from *in vitro* single-fiber work-loop studies, a result which suggests the presence of an elastic energy mechanism. Serial elastic elements on one side of the caudal region of the body could be engaged by activated muscle as the segment is lengthened by the kinetic energy of the traveling undulatory wave. This process would store elastic energy for release as positive mechanical work during the first half of the shortening cycle (Fig. 8). These issues are detailed in the following sections.

The functional significance of altering body stiffness

Because undulatory swimmers propel themselves with a traveling wave of bending, this mechanical process can be understood, in part, using the principles of dynamically bending beams (Long and Nipper, 1996). A mechanical wave travels through a structure at a speed proportional to the square root of its stiffness; if the frequency of the driving force approaches the natural frequency of the structure, the mechanical cost of movement is minimized (Den Hartog, 1956; Timoshenko *et al.*, 1974). Fish, however, do not behave like simple beams—they drive their propulsive body waves over a wide range of frequencies, which varies the hydrodynamic loads

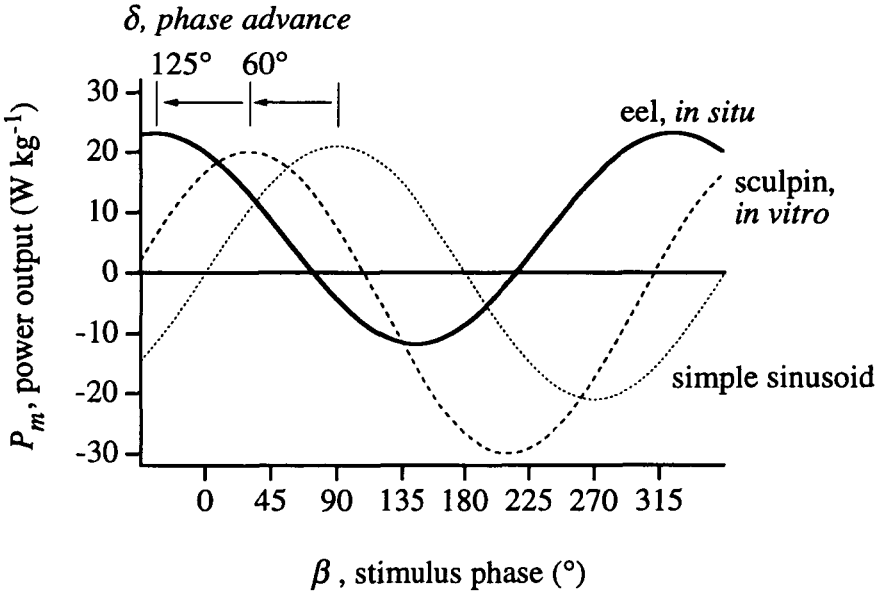

FIG. 7. Muscle power output. The eel *in situ* curve is derived from measurements using the whole-body work loop technique (eq. 20 and Fig. 5B). Maximal net P_m in the *in situ* experiment occurs when $\beta = 325°$ (phase advance, $\delta = 125°$). The sculpin *in vitro* curve is derived from measurements using the single-fiber work loop technique (eq. 21) on isolated white muscle bundles of sculpin (Johnson and Johnston, 1991). Maximal net P_m in the *in vitro* experiment occurs when $\beta = 30°$ ($\delta = 60°$). The simple sinusoid (see eq. 22) assumes that positive net P_m can only by generated during muscle shortening.

on the body and hence the propulsive power. The hydrodynamic loads also vary along the body and through the tailbeat cycle. Given the variable undulatory motion and the resulting changes in hydrodynamic loads, fish probably achieve a wide range of swimming behaviors by altering their body stiffness (Blight, 1977).

As demonstrated by the experiments herein, American eels can triple their body's flexural stiffness (Fig. 3C). Driven by stimulated caudal musculature, body stiffness, EI_{rel}, increases with increases in the net positive muscle work (negative of W_{rel} in Figs. 5C and 6). Changes of this magnitude in EI_{rel} would permit the eel to match the body's natural frequency to the driving frequency over a range of tailbeat frequencies, thus minimizing the internal cost of bending the body during swimming (Long and Nipper, 1996). Furthermore, increases in EI_{rel} would increase the speed at which the undulatory wave travels, a condition required for increased swimming speed in mechanical fish models (McHenry et al. 1995). While changes in unstimulated EI_{rel} alter undulatory motion in live longnose gar (Long *et al.*, 1996), whether EI_{rel} is actively controlled by the caudal muscles during swimming remains untested in any species.

TABLE 2. *Isometric muscle properties of whole-body preparation with 167 msec tetanic stimulus.*

Variable	Mean	St. error
Activation delay, detectable M	17 msec	± 0.0
Time to M_{max}	139 msec	± 34.6
Relaxation time, to 50% M_{max}	330 msec	± 42.4
M_{max}	0.02 Nm	± 0.008

* Sample size = 3 for each value.
** All times are relative to the onset of the electrical stimulus.
*** Electrical stimulus was supra-maximal.

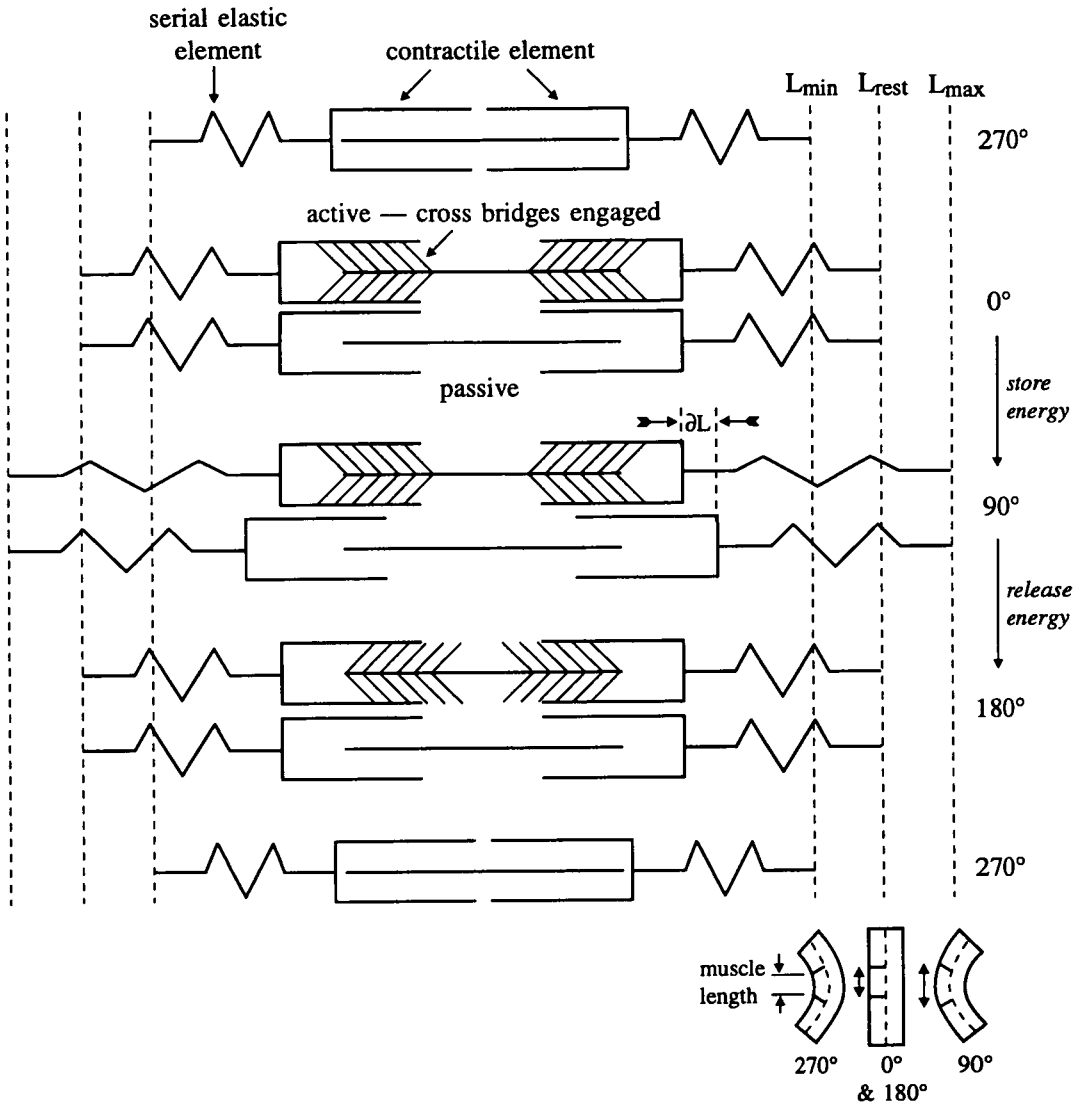

FIG. 8. A conceptual model for elastic energy in undulatory swimmers. The caudal muscles of eel may use elastic energy to power bending and stiffen the body simultaneously. In the absence of local muscle activity (contractile elements figured without cross-bridges), the wave of bending, generated by muscles anteriorly, will propagate down the body, transmitting kinetic energy and causing undulatory motion of the passive system in the caudal region. When caudal muscles are active (figured with cross-bridges attached) with a duty cycle of 50%, they can produce maximal work by engaging their cross-bridges at a time of 0° (segment at resting length and lengthening). The muscle, with cross-bridges engaged, generates high force (1.75 times that of shortening, Altringham *et al.*, 1993) as it resists lengthening caused by the traveling mechanical wave. The muscle engages and strains the more flexible serial elastic elements (SEE), causing them to store elastic energy. At 90° (maximal segment length), the strain in the SEE, and hence the stored elastic energy, is maximal; the extra strain added by muscle activity is indicated (δL). At the next moment, the muscles begin to contract, which keeps the springs engaged in order to release the strain energy and to transmit the positive muscle work now being generated. At 180° (segment at resting length and shortening), the muscle should be inactive, since the SEE will have released the stored energy and will be shortening passively because of the traveling wave of bending.

One way to assess the likelihood that muscles are actively increasing EI_{rel} during swimming is to examine EMG patterns. EMG patterns of American eel from the location closest to the axial position (75% L_b) that I used for whole-body work loops (70% L_b), show a β of 25° for both red and white muscle in 35 to 40 cm long eels swimming at 1 L_b sec^{-1} (Gillis, personal communication). Using this β, the results of this present study predict that live, steadily swimming eels use their caudal musculature to increase EI_{rel} by a factor of up to 1.6 (Fig. 6). This dynamic model of *in situ* muscle function also predicts that the caudal musculature may increase the muscular work output, the negative of W_{rel}, by a factor of up to 4.0 during swimming (Fig. 6). The precise magnitude of the increase in stiffness or muscle work would depend on the number of motor units recruited during swimming. It is important to keep in mind that all of the white (fast) and red (slow) muscle fibers on one side of the body are stimulated with the supra-maximal voltages used in the whole-body work-loop experiments. While eels appear to be unusual, compared to other species, in stimulating both fiber types at all speeds (Grillner and Kashin, 1976), it is unlikely that they recruit all of the fibers of each type at low speeds. More likely is a scenario in which more motor units are recruited as speed increases (Jayne and Lauder, 1996). At faster speeds, β could also decrease and, according to the model (Fig. 6), permit greater muscle power, P_m, and EI_{rel} to be produced. To swim slowly, the model predicts that β would increase.

Muscle activity and body stiffness

From results of *in vitro* work loops on small bundles of the white caudal muscle of saithe, *Pollachius virens,* Altringham *et al.* (1993) predicted that those muscles, when activated while lengthening *in vivo,* would generate maximal force, resulting in "negative" work (see Introduction) locally and internally (a positive W_{ext} or W_{rel}). This local negative work would stiffen the muscles, permitting them to transmit, as functional tendons, mechanical power from the anterior muscle to the caudal propulsive elements (Videler, 1993; Wardle *et al.,* 1995). Thus, I was initially surprised to find the opposite result in the *in situ* whole-body work loop experiments—increased body stiffness was correlated with increased net *positive* muscle work (a negative W_{rel} in Fig. 6). De-coupling of stiffness and work has been found elsewhere—muscle work could not be predicted from muscle force in the pectoral muscle of pumpkinseed sunfish, *Lepomis gibbosus,* stimulated during cyclic strains (Luiker and Stevens, 1991). The unexpected mechanical behavior in the eel whole-body preparation might be explained by comparing the results from *in vitro* and *in situ* work loop experiments with those predicted by a model of simple muscle contraction (Fig. 7).

In the simplest case, myomeric muscles should produce maximal power, P_m, when they are electrically activated at their maximum length (β = 90°) and forcefully shorten for 50% of the cycle (simple sinusoid in Fig. 7). Activation at 90°, however, does not account for the delay between the onset of the stimulus and the actual contraction, which is 17 msec (Table 2). Thus, for cyclic bending at 3 Hz, maximal P_m would require a compensatory phase advance, δ, of 18° in β, yielding a prediction of maximal P_m at β = 72°. *In vitro* measurements of isolated white caudal muscle fibers, however, show production of maximal net muscle work at β = 29° in sculpin, *Myoxocephalus scorpius* (bending frequency of 5 Hz; Johnston *et al.,* 1993), and 36° in dogfish, *Scyliorhinus canicula* (bending frequency of 3.3 Hz; Curtin and Woledge, 1993*a*). I chose the sculpin's value of approximately 30° to represent bony fish (Fig. 7). This β yields a δ of 60° relative to the maximal work predicted by the simple contraction model. Given the 18° needed to engage the contractile elements, that still leaves 42° of muscle activity before shortening begins. By activating the muscles as they are lengthened, this "pre-stretch" period is thought to permit fibers to generate greater force during shortening; longer periods of pre-stretch, *i.e.,* further advances in β, reduce maximal net P_m by increasing the amount of negative work generated locally (Johnson and Johnston, 1991; Johnston,

1991; but see Lombardi *et al.*, 1995). *In situ* measurements of white and red caudal muscle show even greater δ than that of the *in vitro* models; eel muscle produces maximal P_m at β = 325°, a δ of 125° (Fig. 7).

An elastic energy model for undulatory swimmers

The whole-body preparation produced maximal net P_m when it was stimulated one-third of the way through the muscles' lengthening cycle (β = 325°), which begins and ends at 270° and 90°, respectively. Since, by definition, *instantaneous* positive P_m can only occur when muscle force is generated during shortening (displacement during shortening is positive and during lengthening is negative), a *net* positive P_m at β = 325° means that, even though muscle stimulation occurs during lengthening, most of the muscle force is effectively applied during shortening. How can this be? How can force applied during one part of the cycle be delayed and then released during another?

One explanation of this behavior is that the caudal muscle of eels stores energy in serial elastic elements (SEE). I propose that the caudal muscles generate positive net P_m by loading the SEE as an external load attempts to lengthen the muscle; the load external to the segment in question is provided by the kinetic energy of the traveling wave of bending (Fig. 8). As long as the active contractile elements are stiffer than the SEE (Alexander, 1988), the SEE would be stretched more during lengthening, compared to when the contractile elements are inactive, and could then release the stored strain energy during the shortening phase. In this way, the caudal body segments would produce a net positive P_m even though the muscle had been activated during a large portion of the segment's lengthening cycle. In addition, muscles would function as *dynamic springs,* stiffening the body by increasing the force needed to lengthen that segment and by increasing the strain in the SEE. Increased strain tends to stiffen visco-elastic structures (*e.g.,* Hebrank, 1980; Long, 1992).

Which structures function as the SEE? Unfortunately, we do not adequately understand the ultrastructure of fish muscle and connective tissues to make a sensible conjecture. In a review of structures that transmit force in the muscle of amphibians, birds, and mammals, Trotter (1993) found evidence that the entire surface of a muscle fiber may transfer tension to the endomysium, which, in turn, transfers shear force between discontinuous muscle fibers. If analogous structures are found in eel muscles, then the endomysium might function proximally as the SEE required by the elastic energy model. On a gross level, adjacent myotomes may function as SEE, since they are arranged serially (Westneat *et al.,* 1993) and are activated sequentially (Jayne and Lauder, 1995*a*); anterior myotomes activated earlier in the tailbeat cycle might stiffen and act as SEE for caudal myotomes newly activated. Other structures to which myomeric muscles attach, and which therefore may function as SEE, include the skin (Hebrank, 1980; Long *et al.,* 1996; Wainwright *et al.,* 1978) and the axial skeleton (Long, 1992, 1995).

How might the elastic energy model be tested? While the whole-body work-loop results on eel suggested the model in the first place, they permit a simple test of internal consistency. According to the elastic energy model (Fig. 8), I can predict that with a duty cycle of 50%, muscle should be active (cross-bridge activity) at β = 0°, since activity before then will merely pull on SEE that are slack. Furthermore, the muscle should stay active until 180°, since release before then will not allow SEE to transfer stored strain energy to surrounding structures. To predict optimal EMG β, one must know the delay between electrical onset and cross-bridge activity. Eel muscles have a contraction delay of 17 msec (Table 2) or 18°. Thus, I would predict that eels would produce maximal P_m when β = 342° (360°–18°). I measured maximal net P_m at a closely-corresponding β = 325° in the whole-body work loop experiments (Fig. 7). Both theoretical and measured values of β that produce maximal net P_m predict that EMG β would occur early in the lengthening portion of the bending cycle. Clearly, the model must be tested in live eels. We know already that at relatively slow swim-

ming speeds of 1.0 L_b sec^{-1}, $\beta = 25°$ in the mid-caudal muscles (Gillis, personal communication), a result which suggests the following testable prediction—during faster steady swimming, or vigorous unsteady swimming, when more P_m and higher EI are required, EMG β should decrease from 25° towards 342°. Shifts in the opposite direction would refute the model.

Because this is first time, to my knowledge, that a specific elastic energy mechanism has been proposed for the myotomal muscle of undulatory swimmers, it is important to carefully consider potential problems (questions 1 through 5, below). The reader should keep in mind that the experiments conducted in this study included only a single bending frequency (3 Hz), a single muscle strain (±4%), a single body position (70% L_b), and a single temperature (20°C). While these values are physiological, all four of these variables significantly alter dynamic muscle properties in *in vitro* single-fiber experiments. Thus, extensions of the elastic energy model, and results of the *in situ* whole-body experiments in general, should be taken cautiously.

(1) What provides the load needed to strain activated muscle and SEE? In a terrestrial, limbed vertebrate, the load needed to strain SEE is provided, in part, by gravitational force, which, in the form of potential energy, is exchanged for kinetic energy which, in turn, is converted to strain energy in stretched connective tissues (*e.g.,* Farley *et al.,* 1991; McMahon, 1985). On the other hand, neutrally-buoyant swimming vertebrates have no external force which might load elastic elements; any energy used in lengthening muscle and elastic elements must be provided locally by P_m from muscles in other locations. This condition is problematic, since the P_m used for lengthening would be unavailable at that moment for hydrodynamic power and, considering losses during transmission, a substantial benefit would be needed to compensate. While some compensation might be provided by the greater forces generated as muscle is lengthened (see question 2 below), those greater forces require greater antagonistic force in turn. My counter argument is this: the "external" loading could be supplied, caudally, by the kinetic energy of the traveling wave of bending, which transfers work from anterior to posterior body segments. This mechanical wave will travel caudally without input from the caudal muscles (Blight, 1977; Long *et al.,* 1994; Wassersug and Hoff, 1985); it propagates by exchanging strain and kinetic energy in elastic structures (McHenry *et al.,* 1995). *The traveling wave of bending and its kinetic energy is thus the undulatory analogue to gravity and its potential energy.* The elastic elements and the caudal muscle harness this propagating energy to strain tissues and lengthen muscle. In turn, the newly-loaded body section transfers its locally-generated P_m caudally to other segments and to the surrounding fluid. Kinetic and strain energy are thus cyclically exchanged in a manner partially analogous to that seen in the limbed locomotion of vertebrates.

(2) Why should muscles use elastic energy when they can generate power directly and presumably with greater efficiency? Given that elastic tissues dissipate some of the stored strain energy (see Alexander, 1988), the mechanical "reason" to store elastic energy from the traveling wave of bending is that muscle can produce 1.75 times the force of shortening as it is caused to lengthen (Altringham *et al.,* 1993; also see McMahon, 1985). The "pay-off" threshold for elastic return would therefore be efficiencies (ratio of energy returned to energy stored) greater than 57% (ratio of shortening and lengthening forces). The efficiency of the tendon in wallaby, *Macropus rufogriseus,* is about 93% (Ker *et al.,* 1986); the efficiency of the intervertebral joints of blue marlin, *Makaira nigricans,* is over 90% as well (Long, 1992). While the functional SEE in eel have not been identified, it is clear that vertebrate connective tissues can have efficiencies that would render feasible the elastic energy model of caudal muscle function. If the caudal muscles use elastic energy to produce greater amounts of P_m than they could by simple shortening, it leaves us with the intriguing possibility that this mechanism compensates for the reduced muscle mass as the

body tapers caudally. The elastic energy mechanism might also compensate for P_m production limitations that would constrain actively shortening muscle to operate at ratios of contraction velocity to maximal contraction velocity near 0.2 to 0.3 (see Rome *et al.,* 1988); caudal muscle fibers could specialize in high force production without compromising production of positive work, a capacity that would extend the range of the eel's undulatory behaviors.

(3) Do whole-body work loop experiments produce realistic muscle properties? Assuming that most of the caudal muscle mass in eels is white (fast), the maximal net P_m for the caudal musculature of eel (23 W kg^{-1}, Fig. 7) is similar to that measured in a variety of species using the *in vitro* single fiber method: 20 to 25 W kg^{-1} in precaudal white muscle of sculpin (Johnson and Johnston, 1991), 31 W kg^{-1} in caudal white muscle of scup (Rome *et al.,* 1993), 20 W kg^{-1} in caudal white muscle of Antarctic rock cod (Franklin and Johnston, 1997), and 31 W kg^{-1} in caudal white muscle of saithe (Altringham *et al.,* 1993). This close correspondence supports the contention that the whole-body work-loop method accurately measures net muscle power output under dynamic loading conditions that simulate certain aspects of *in vivo* conditions. However, the results from the *in situ* whole-body method deviate from those of the *in vitro* studies in one important aspect—the timing of stimulus onset, β, that produces maximal P_m (see δ in Fig. 7). This is exactly the kind of difference that we would expect when comparing a system without SEE (*in vitro* work loops) to one with SEE (*in situ* work loops).

(4) How realistic are the stimulus parameters? Because I was interested in the maximal performance of this system, all of the red and white muscles were activated. While this pattern may be realistic for steadily swimming eels (Grillner and Kashin, 1976), it has been described in other species only during unsteady kick-and-glide and fast-start behaviors (see Jayne and Lauder, 1996). A potential problem is that direct electrical stimulation of the muscles may have also stimulated afferent neural pathways that were not destroyed in the whole-body preparation; these pathways could provide feedback to the central pattern generators in the spinal cord which could, in turn, stimulate motor units independently (see Fetcho, 1987; Fetcho and Faber, 1988). Gray (1936*a, b*) found that spinally-transected eels, such as the ones used in this study, were inhibited from muscle contractions in response to tactile stimulation by strong restraint of the body, which is a condition similar to that imposed by the bending grips in the experimental machine. It is possible, although untested, that this inhibitory mechanism may have effectively blocked the response to afferent stimulation at the level of the central pattern generator or motor pathway.

(5) How accurately do the whole-body work loops simulate the mechanical conditions seen in life? Because a small section of the intact body was isolated and bent, these experiments analyzed locally what is in life part of the integrated locomotor system consisting of a temporal and spatial series of internally and externally coupled mechanical events. Ideally, and unrealistically given our present knowledge, all of these mechanical conditions should be satisfied simultaneously in the *in situ* experiments. Clearly, they are not—the entire body is not bending, adjacent muscle activity is simultaneous not sequential, and the external hydrodynamic forces are not present on the bending section. While not ideal, the whole-body method is the first, to my knowledge, to simultaneously combine the conditions of muscle operating (a) attached to intact SEE, (b) in alternating left- and right-side contractions, (c) with stimulation at different times relative to its strain, (d) as the body is bent sinusodially by an anterior wave generator, and (e) under conditions in which the dynamic stiffness, damping, and work required to bend the body are measured.

In summary, results from the whole-body work loop experiments on eels suggest an integrated view of swimming mechanics and caudal muscle function. The muscles generate force as that side of the body is lengthened to produce, simultaneously, net positive mechanical work and increased

body stiffness. The dual function of caudal muscle as a body bender and dynamic stiffener is made possible by the use of elastic energy to store and release muscle work. Increases in body stiffness will increase the speed of the traveling wave of bending and make bending itself less mechanically costly at higher tail-beat frequencies. By examining dynamic, time-dependent behaviors of the muscles operating within the intact body, this integrated view emerges—of function at different structural levels, from single sarcomeres to contiguous blocks of myomeres with their associated elastic elements—a perspective unanticipated from any single level.

ACKNOWLEDGMENTS

I would like to thank John Bertram and Richard Marsh for organizing this symposium and inviting me to participate. Karen Nipper was instrumental in helping to design the whole-body work loop technique, the inspiration for which was originally provided by conversations with Thelma Williams and Ted Goslow. John Hermanson provided neurobiological advice. Wayne Gilchrest graciously provided the eels. William Shepherd and Gary Gillis kindly shared their unpublished data on eel swimming kinematics and electromyography, respectively. Robert Suter and Matt McHenry critiqued earlier versions of this manuscript. Later versions were helped by Bruce Jayne and an anonymous reviewer. This work was funded by grant number N0014-97-1-0292 to J.H.L. from the Office of Naval Research.

REFERENCES

Alexander, R. M. 1988. *Elastic mechanisms in animal movement.* Cambridge University Press, New York.

Altringham, J. D. and I. A. Johnston. 1990. Scaling effects on muscle function: Power output of isolated fish muscle fibers performing oscillatory work. J. exp. Biol. 151:453–467.

Altringham, J. D., C. S. Wardle, and C. I. Smith. 1993. Myotomal muscle function at different locations in the body of a swimming fish. J. exp. Biol. 182: 191–206.

Bennett, M. B., R. F. Ker, and R. M. Alexander. 1987. Elastic properties of structures in the tails of cetaceans (*Phocoena* and *Lagenorhynchus*) and their effect on the energy cost of swimming. J. Zool., Lond., 211:177–192.

Blickhan, R. and J.-Y. Cheng. 1994. Energy storage by elastic mechanisms in the tail of large swimmers—a re-evaluation. J. theor. Biol. 168:315–321.

Blight, A. R. 1977. The muscular control of vertebrate swimming movements. Biol. Rev. 52:181–218.

Bowtell, G. and T. Williams. 1991. Anguilliform body dynamics: Modeling the interaction between muscle activation and body curvature. Phil. Trans. R. Soc., Lond. B. 334:385–390.

Cheng, J.-Y. and R. Blickhan. 1994. Bending moment distribution along swimming fish. J. theor. Biol. 168:337–348.

Coughlin, D. J. and L. C. Rome. 1996. The roles of pink and red muscle in powering steady swimming in scup, *Stenotomus chrysops.* Amer. Zool. 36:666–677.

Coughlin, D. J., G. Zhang, and L. C. Rome. 1996. Contraction dynamics and power production of pink muscle of the scup (*Stenotomus chrysops*). J. exp. Biol. 199:2703–2712.

Curtin, N. A. and R. C. Woledge. 1993*a*. Efficiency of energy conversion during sinusoidal movement of white muscle fibres from the dogfish *Scyliorhinus canicula.* J. exp. Biol. 183:137–147.

Curtin, N. A. and R. C. Woledge. 1993*b*. Efficiency of energy conversion during sinusoidal movement of red muscle fibers from the dogfish *Scyliorhinus caniculua.* J. exp. Biol. 185:195–206.

Den Hartog, J. P. 1956. *Mechanical vibrations.* 4th ed. McGraw-Hill, New York.

Dial, K. P. 1992. Activity patterns of the wing muscles of the pigeon (*Columbia livia*) during different modes of flight. J. Exp. Zool. 262:357–373.

Ettema, G. J. C. 1996. Mechanical efficiency and efficiency of storage and release of series elastic energy in skeletal muscle during stretch-shorten cycles. J. exp. Biol. 199(9):1983–1997.

Farley, C. T., R. Blickhan, J. Saito, and C. R. Taylor. 1991. Hopping frequency in humans: A test of how springs set stride frequency in bouncing gaits. J. Appl. Physiol. 71(6):2127–2132.

Fetcho, J. R. 1987. A review of the organization and evolution of motoneurons innervating the axial musculature of vertebrates. Brain Res. Rev. 12(1987):243–280.

Fetcho, J. R. and D. S. Faber. 1988. Identification of motoneurons and interneurons in the spinal network for escapes initiated by the mauthner cell in goldfish. J. Neurosci. 8(11):4192–4213.

Franklin, C. E. and I. A. Johnston. 1997. Muscle power output during escape responses in an Antarcttic fish. J. exp. Biol. 200:703–712.

Gillis, G. B. 1996. Undulatory locomotion in elongate aquatic vertebrates: Anguilliform swimming since Sir James Gray. Amer. Zool. 36:656–665.

Gray, J. 1933. Studies in animal locomotion. I. The movement of fish with special reference to the eel. J. exp. Biol. 10:88–104.

Gray, J. 1936*a*. Studies in animal locomotion. IV. The neuromuscular mechanism of swimming in the eel. J. exp. Biol. 13:170–180.

Gray, J. 1936*b*. Studies in animal locomotion. V. Resistance reflexes in the eel. J. exp. Biol. 13:181–191.

Grillner, S. and S. Kashin. 1976. On the generation and performance of swimming in fish. *In* R. M. Herman, S. Grillner, P. S. G. Stein, and D. G. Stuart (eds.), Neural control of locomotion, pp. 181–201. Plenum Press, New York.

Hebrank, M. R. 1980. Mechanical properties and locomotor functions of eel skin. Biol. Bull. 158:58–68.

Hess, F. and J. J. Videler. 1984. Fast continuous swimming of saithe (*Pollachius virens*): A dynamic analysis of bending moments and muscle power. J. exp. Biol. 109:229–251.

Jayne, B. C. and G. V. Lauder. 1993. Red and white muscle activity and kinematics of the escape response of the bluegill sunfish during swimming. J. Comp. Physiol. A. 173:495–508.

Jayne, B. C. and G. V. Lauder. 1994. How swimming fish use slow and fast muscle fibers: Implications for models of vertebrate muscle recruitment. J. Comp. Physiol. A. 175:123–131.

Jayne, B. C. and G. V. Lauder. 1995*a*. Are muscle fibers within fish myotomes activated synchronously? Patterns of recruitment within deep myomeric musculature during swimming in largemouth bass. J. exp. Biol. 198:805–815.

Jayne, B. C. and G. V. Lauder. 1995*b*. Red muscle motor patterns during steady swimming in largemouth bass: Effects of speed and correlations with axial kinematics. J. Exp. Biol. 198:1575–1587.

Jayne, B. C. and G. V. Lauder. 1996. New data on axial locomotion in fishes: How speed affects diversity of kinematics and motor patterns. Amer. Zool. 36(6):642–655.

Johnson, T. P. and I. A. Johnston. 1991. Power output of fish muscles fibres performing oscillatory work: Effects of acute and seasonal temperature change. J. exp. Biol. 157:409–423.

Johnson, T. P., D. A. Syme, B. C. Jayne, G. V. Lauder, and A. F. Bennett. 1994. Modeling red muscle power output during steady and unsteady swimming in largemouth bass. Am. J. Physiol. 267: R481–R488.

Johnsrude, C. L. and P. W. Webb. 1985. Mechanical properties of the myotomal musculo-skeletal system of rainbow trout, *Salmo gairdneri*. J. exp. Biol. 119:71–83.

Johnston, I. A., C. E. Franklin, and T. P. Johnson. 1993. Recruitment patterns and contractile properties of fast muscle fibres isolated from rostral and caudal myotomes of the short-horned sculpin. J. exp. Biol. 185:251–265.

Johnston, I. A., J. L. Van Leeuwen, M. L. F. Davies, and T. Beddow. 1995. How fish power predation fast starts. J. exp. Biol. 198:1851–1861.

Jordan, C. E. 1996. Coupling internal and external mechanics to predict swimming behavior: A general approach? Amer. Zool. 36(6):710–722.

Josephson, R. K. 1985. Mechanical power output from striated muscle during cyclic contractions. J. exp. Biol. 114:93–512.

Ker, R. F., N. J. Dimery, and R. M. Alexander. 1986. The role of tendon elasticity in hopping in a wallaby (*Macropus rufogriseus*). J. Zool. Lond. A. 208:417–428.

Lighthill, M. J. 1975. *Mathematical biofluiddynamics*. Res. Conf. Nat. Sci. Found., 1973, New York Soc. Ind. Appl. Math. SIAM.

Lombardi, V., G. Piazzesi, M. A. Ferenczi, H. Thirlwell, I. Dobbie, and M. Irving. 1995. Elastic distortion of myosin heads and repriming of the working stroke in muscle. Nature 374:553–555.

Long, J. H., Jr. 1992. Stiffness and damping forces in the intervertebral joints of blue marlin (*Makaira nigricans*). J. exp. Biol. 162:131–155.

Long, J. H., Jr. 1995. Morphology, mechanics and locomotion: The relation between the notochord and swimming motions in sturgeon. Env. Biol. Fishes 44:199–211.

Long, J. H., Jr., M. E. Hale, M. J. McHenry, and M. W. Westneat. 1996. Functions of fish skin: The mechanics of steady swimming in longnose gar, *Lepisosteus osseus*. J. exp. Biol. 199:2139–2151.

Long, J. H., Jr., M. J. McHenry, and N. C. Boetticher, N. C. 1994. Undulatory swimming: How traveling waves are produced and modulated in sunfish (*Lepomis gibbosus*). J. exp. Biol. 192:129–145.

Long, J. H., Jr. and K. S. Nipper. 1996. The importance of body stiffness in undulatory propulsion. Amer. Zool. 36(6):678–694.

Luiker, E. A. and E. D. Stevens. 1991. Effect of stimulus frequency and duty cycle on force and work in fish muscle. Can J. Zool. 70:1135–1139.

McHenry, M. J., C. A. Pell, and J. H. Long, Jr. 1995. Mechanical control of swimming speed: Stiffness and axial wave form in undulating fish models. J. exp. Biol. 198(11):2293–2305.

McMahon, T. A. 1985. The role of compliance in mammalian running gaits. J. exp. Biol. 115:263–282.

Pabst, D. A. 1996. The role of elastic energy storage in aquatic locomotion. Amer. Zool. 36(6):723–735.

Rome, L. C., R. P. Funke, R. M. Alexander, G. Lutz, H. Aldridge, F. Scott, and M. Freadman. 1988. Why animals have different muscle fibre types. Nature 335:824–827.

Rome, L. C. and D. Swank. 1992. The influence of temperature on power output of scup red muscle during cyclic length changes. J. exp. Biol. 171: 261–281.

Rome, L. C., D. Swank, and D. Corda. 1993. How fish power swimming. Science 261:340–343.

Spierts, I. L. Y., H. A. Akster, I. H. C. Vos, and J. W. M. Osse. 1996. Local differences in myotendinous junctions in axial muscle fibres of carp (*Cyprinus carpio* L.). J. exp. Biol. 199:825–833.

Stevens, K. K. 1987. *Statics and strength of materials*. 2nd. ed. Prentice-Hall, Englewood Cliffs, New Jersey.

Swank, D. M., G. Zhang, and L. C. Rome. 1997. Contraction kinetics of red muscle in scup: Mechanism for variation in relaxation rate along the length of the fish. J. exp. Biol. 200:1297–1307.

Timoshenko, S., D. H. Young, and W. Weaver, Jr.

1974. *Vibration problems in engineering.* 4th ed. John Wiley and Sons, New York.

Trotter, J. A. 1993. Functional morphology of force transmission in skeletal muscle. Acta Anat. 146: 205–222.

Van Leeuwen, J. L., M. J. M. Lankeet, H. A. Akster, and J. W. M. Osse. 1990. Function of red muscles of carp (*Cyprinus carpio*): Recruitment and normalized power output during swimming in different modes. J. Zool. Lond. 220:123–145.

Videler, J. J. 1993. *Fish swimming.* Chapman and Hall, New York.

Wainwright, S. A., F. Vosburgh, and J. H. Hebrank. 1978. Shark skin: Function in locomotion. Science 202:747–749.

Wardle, C. S., J. J. Videler, and J. D. Altringham. 1995. Tuning in to fish swimming waves: Body form, swimming mode and muscle function. J. exp. Biol. 198(8): 1629–1636.

Wassersug, R. J. and K. v. S. Hoff. 1985. The kinematics of swimming in anuran larvae. J. exp. Biol. 119:1–30.

Westneat, M. W., W. Hoese, C. A. Pell, and S. A. Wainwright. 1993. The horizontal septum: Mechanisms of force transfer in locomotion of scombrid fishes (Scombridae, Perciformes). J. Morph. 217:183–204.

Wilkinson, L. 1989. *SYSTAT: the system for statistics.* SYSTAT, Inc., Evanston, IL.

Williams, T. L., S. Grillner, V. V. Smoljaninov, P. Wallen, S. Kashin, and S. Rossignol. 1989. Locomotion in lamprey and trout: The relative time of activation and movement. J. exp. Biol. 143:559–566.

Corresponding Editor: Todd Gleason